

A Method for Calculating Transient Surface Temperatures and Surface Heating Rates for High-Speed Aircraft

*Robert D. Quinn
Analytical Services and Materials, Inc.
Edwards, California*

*Leslie Gong
NASA Dryden Flight Research Center
Edwards, California*

The NASA STI Program Office...in Profile

Since its founding, NASA has been dedicated to the advancement of aeronautics and space science. The NASA Scientific and Technical Information (STI) Program Office plays a key part in helping NASA maintain this important role.

The NASA STI Program Office is operated by Langley Research Center, the lead center for NASA's scientific and technical information. The NASA STI Program Office provides access to the NASA STI Database, the largest collection of aeronautical and space science STI in the world. The Program Office is also NASA's institutional mechanism for disseminating the results of its research and development activities. These results are published by NASA in the NASA STI Report Series, which includes the following report types:

- **TECHNICAL PUBLICATION.** Reports of completed research or a major significant phase of research that present the results of NASA programs and include extensive data or theoretical analysis. Includes compilations of significant scientific and technical data and information deemed to be of continuing reference value. NASA's counterpart of peer-reviewed formal professional papers but has less stringent limitations on manuscript length and extent of graphic presentations.
- **TECHNICAL MEMORANDUM.** Scientific and technical findings that are preliminary or of specialized interest, e.g., quick release reports, working papers, and bibliographies that contain minimal annotation. Does not contain extensive analysis.
- **CONTRACTOR REPORT.** Scientific and technical findings by NASA-sponsored contractors and grantees.
- **CONFERENCE PUBLICATION.** Collected papers from scientific and technical conferences, symposia, seminars, or other meetings sponsored or cosponsored by NASA.
- **SPECIAL PUBLICATION.** Scientific, technical, or historical information from NASA programs, projects, and mission, often concerned with subjects having substantial public interest.
- **TECHNICAL TRANSLATION.** English-language translations of foreign scientific and technical material pertinent to NASA's mission.

Specialized services that complement the STI Program Office's diverse offerings include creating custom thesauri, building customized databases, organizing and publishing research results...even providing videos.

For more information about the NASA STI Program Office, see the following:

- Access the NASA STI Program Home Page at <http://www.sti.nasa.gov>
- E-mail your question via the Internet to help@sti.nasa.gov
- Fax your question to the NASA Access Help Desk at (301) 621-0134
- Telephone the NASA Access Help Desk at (301) 621-0390
- Write to:
NASA Access Help Desk
NASA Center for AeroSpace Information
7121 Standard Drive
Hanover, MD 21076-1320



A Method for Calculating Transient Surface Temperatures and Surface Heating Rates for High-Speed Aircraft

Robert D. Quinn
Analytical Services and Materials, Inc.
Edwards, California

Leslie Gong
NASA Dryden Flight Research Center
Edwards, California

National Aeronautics and
Space Administration

Dryden Flight Research Center
Edwards, California 93523-0273

NOTICE

Use of trade names or names of manufacturers in this document does not constitute an official endorsement of such products or manufacturers, either expressed or implied, by the National Aeronautics and Space Administration.

Available from the following:

NASA Center for AeroSpace Information (CASI)
7121 Standard Drive
Hanover, MD 21076-1320
(301) 621-0390

National Technical Information Service (NTIS)
5285 Port Royal Road
Springfield, VA 22161-2171
(703) 487-4650

ABSTRACT

This report describes a method that can calculate transient aerodynamic heating and transient surface temperatures at supersonic and hypersonic speeds. This method can rapidly calculate temperature and heating rate time-histories for complete flight trajectories. Semi-empirical theories are used to calculate laminar and turbulent heat transfer coefficients and a procedure for estimating boundary-layer transition is included. Results from this method are compared with flight data from the X-15 research vehicle, YF-12 airplane, and the Space Shuttle Orbiter. These comparisons show that the calculated values are in good agreement with the measured flight data.

NOMENCLATURE

a	speed of sound, ft/sec
Btu	British thermal units
c_1, c_2, c_3, c_4, c_5	defined by equations 38 through 42
CFD	computational fluid dynamics
C_f	local skin friction coefficient
C_M	transition Mach number coefficient
$C_{p,w}$	specific heat of wall material, Btu/lbm °R
DFRC	Dryden Flight Research Center, Edwards, California
f	function
F	empirical factor in transient heating and heat transfer coefficient equations
F.S.	fuselage station
g	gravitational conversion factor, 32.17 lbm ft/lb sec ²
h	heat transfer coefficient, lbm/ft ² sec
H	enthalpy, Btu/lbm
J	mechanical equivalent of heat, 778 ft lb/Btu
K	radiation geometry factor 1.0
m	exponent in friction law
M	Mach number
N	reciprocal exponent in velocity profile power law
P_L	static pressure at edge of boundary layer, lb/ft ²
P_{st}	stagnation pressure, lb/ft ²
P_1	static pressure in front of shock, lb/ft ²
Pr	Prandtl number
q	heat flux, Btu/ft ² sec

q/q_0	ratio of circumferential heat flux on a sphere or cylinder to the stagnation point heat flux
r	radius of body of revolution, ft
R	radius of nose or leading edge, ft
R	gas constant for air, 53.3 ft lb/lbm °R
RA	modified Reynolds analogy factor
Re	Reynolds number, $\frac{\rho V x}{\mu}$
Re_t	transition Reynolds number, $\frac{\rho V x}{\mu}$
$R\theta$	Reynolds number based on momentum thickness, $\frac{\rho V \theta}{\mu}$
S	solar and nocturnal radiation input, Btu/ft ² sec
SB	speed brake
ST	Stanton number, $h/\rho V$
t	time, sec
T	temperature
T_{st}	stagnation temperature, °R
T_w	wall or skin temperature, °R
\dot{T}_w	rate of change of wall temperature, °R/sec
V	velocity, ft/sec
$W.S.$	wing station
x	flow distance, ft
β	radiation factor, $\sigma \epsilon K$, Btu/ft ² sec °R ⁴
γ	ratio of specific heats
δ	boundary-layer velocity thickness, ft
ϵ	emissivity
Z	compressibility factor in the thermal equation of state for air
θ	boundary-layer momentum thickness, ft
θ_s	circumferential angle for a cylinder or sphere from stagnation line, deg
Λ	leading edge sweep angle, deg
μ	dynamic viscosity, lbm/ft sec
ρ	density of air, lbm/ft ³
ρ_w	density of wall material, lbm/ft ³
σ	Stefan-Boltzman constant, 4.758×10^{-13} Btu/ft ² sec °R ⁴
τ	wall or skin thickness, ft

ϕ	circumferential angle for a cone, zero on cone center line, deg
$\left(\frac{du}{dx}\right)_{x=0}$	stagnation velocity gradient, 1/sec

Subscripts

L	local flow conditions in the inviscid shear layer or at the edge of the boundary layer
R	boundary-layer recovery
st	stagnation
w	wall
2	conditions behind normal shock

Superscripts

*	evaluate at the reference enthalpy
---	------------------------------------

INTRODUCTION

The Dryden Flight Research Center (DFRC) Edwards, California, conducts flight research on new and advanced high-speed aircraft. Dryden also conducts ground research on new and unique hot structures concepts in the Flight Loads Research Laboratory. The ability to reliably calculate time histories of transient aerodynamic heating rates and surface temperatures is essential to conduct this research and to ensure flight safety.

The best method for predicting aerodynamic heating is viscous computational fluid dynamics (CFD) solutions (refs. 1 and 2). This method provides a direct means of computing heat flux as well as interactions between inviscid and viscous flow regions due to heat transfer and entropy-layer swallowing. However, these methods require large computer run times and storage, and each time the flight conditions change (e.g. the Mach number, altitude and angle of attack) a new computer run must be made. Therefore, using CFD to calculate complete time histories of transient temperatures and heat flux becomes very expensive and time consuming. Further, for turbulent flow the accuracy of viscous CFD solutions is suspect due to the required use of empirical turbulent models.

Consequently, the use of viscous CFD solutions for calculating time histories of transient surface temperatures and aerodynamic heat flux is not feasible, and recourse to approximate aerodynamic heating methods is necessary. To meet these requirements for calculating transient surface temperatures and heat flux to conduct flight and laboratory research, an aerodynamic heating program called TPATH has been developed. This program was originally developed to predict aerodynamic heating for flight safety and flight research on the X-15 research airplane. Subsequently, this program has been used to predict transient surface temperatures and heating rates on all high speed flight vehicles flown at DFRC, including but not limited to the YF-12, SR-71, Space Shuttle, TU-144, Pegasus Hypersonic Experiment, and Hyper-X.

This paper presents the heating methods used in this program and the methodology used to calculate transient surface temperatures and surface heat flux for supersonic and hypersonic aircraft. The results are compared to flight data from the X-15 research airplane, the YF-12 airplane and the space shuttle orbiter.

TRANSIENT AERODYNAMIC HEATING

An aerodynamic heating program called TPATH has been developed at DFRC that is capable of quickly and reliably calculating time histories of transient surface temperatures and surface heat flux at supersonic and hypersonic speeds. This program uses approximate convective-heating methods to predict transient surface temperature and heating rates for three-dimensional stagnation points, for two-dimensional stagnation points with and without sweep, and for laminar and turbulent values with transition for flat plates, wedges and cones. A detailed description of these methods together with the methodology used to apply these approximate methods to supersonic and/or hypersonic vehicles to obtain reliable results is described below.

Stagnation Point

This section discusses transient heating equations and the heat transfer coefficient equations. These are the equations used to calculate stagnation point heating.

Transient Heating Equations

The equation used to calculate surface temperatures and heat flux for three-dimensional stagnation points and two-dimensional stagnation points without sweep is (ref. 3)*

$$q = (\rho_w C p_w \tau) \dot{T}_w = F(h)(H_{st} - H_w) - \beta T_w^4 + S \quad (1)$$

and for two-dimensional stagnation points with sweep is

$$q = (\rho_w C p_w \tau) \dot{T}_w = F(h)(H_R - H_w) - \beta T_w^4 + S \quad (2)$$

The S in equation 1 and 2 is for solar and nocturnal radiation input if required. This term is negligible except for low-speed flow and is normally set equal to zero. The term βT_w^4 is the heat lost by radiation from the surface of the aircraft to the atmosphere.

To obtain good surface temperatures and accurate heat flux, proper engineering judgment must be exercised in determining the heat capacity $(\rho_w C p_w \tau)$ for the surface. Since the values of the specific heat $(C p_w)$ and density (ρ_w) are thermal properties of the material, the only way to significantly vary the heat capacity is to change the material thickness (τ) . For metallic leading edges with thickness up to

*This equation is sometimes referred to as the thin-skin heat balance equation, and describes the heat balance where the surface is represented by a single lump with a heat capacity of $(\rho_w C p_w \tau)$.

0.1 inches, equations 1 or 2 will produce satisfactory results. For material thickness greater than 0.1 inches the following approximations should be used:

For surface temperature rise rates \dot{T}_w equal to or less than 10 °R/sec

$$\bar{\tau} = \tau_0 + 0.5\tau_1$$

where $\tau_0 = 0.1$ inches, $\tau_1 = (\tau - \tau_0)$, τ = actual thickness and $\bar{\tau}$ = equivalent thickness.

For surface temperature rise rates \dot{T}_w greater than 10 but less than 20 °R/sec

$$\bar{\tau} = \tau_0 + 0.4\tau_1$$

For \dot{T}_w greater than 20 but less than 40 °R/sec

$$\bar{\tau} = \tau_0 + 0.3\tau_1$$

and for \dot{T}_w greater than 40 °R/sec

$$\bar{\tau} = \tau_0 + 0.2\tau_1$$

For metallic leading edges with thicknesses greater than 0.2 inches, it may be necessary to perform a thermal analysis to verify the results.

For surfaces that are insulated with low conductivity insulation (e.g. the space shuttle), a material thickness should be used that will result in a heat capacity of approximately 0.1 Btu/ft² °R.

Heat Transfer Coefficients

To solve equations 1 and 2, the heat transfer coefficient (h) must be determined. In the TPATH program, the heat transfer coefficients are calculated by the method of Fay and Riddell (ref. 4) for three-dimensional stagnation points. The method of Beckwith (ref. 5) is used for two-dimensional stagnation points with or without sweep. The equation given by Fay and Riddell for a Lewis number of 1.0 (no dissociation) and a Prandtl number of 0.71 may be written as

$$h = 0.94(\rho_{st}\mu_{st})^{0.4}(\rho_w\mu_w)^{0.1} \sqrt{\left(\frac{du}{dx}\right)_{x=0}} \quad (3)$$

and the equation given by Beckwith for a Lewis number of 1.0 and a Prandtl number of 0.71 may be written as

$$h = 0.704(\rho_{st}\mu_{st})^{0.44}(\rho_w\mu_w)^{0.06} \sqrt{\left(\frac{du}{dx}\right)_{x=0}} \quad (4)$$

The velocity gradient $\left(\frac{du}{dx}\right)_{x=0}$ is given by

$$\left(\frac{du}{dx}\right)_{x=0} = \frac{1}{R} \sqrt{\frac{2(P_{st} - P_1)g}{\rho_{st}}} \quad (5)$$

and the stagnation enthalpy H_{st} for three-dimensional flow and two-dimensional flow with no sweep is calculated by the following equation:

$$H_{st} = H_2 + \frac{V_2^2}{2gJ} \quad (6)$$

where the subscript “2” denotes conditions calculated behind the normal shock. The wall enthalpy H_w is given by $H_w = f(T_w, P_L)$ and is determined from real gas tables obtained from ref. 6. For two-dimensional flow with sweep, the recovery enthalpy is computed by the following equation:

$$H_R = H_2 + \frac{V_2^2}{2gJ} + 0.855 \frac{V_1^2 \sin^2 \Lambda}{2gJ} \quad (7)$$

where the subscript “2” denotes conditions behind the swept normal shock, and 0.855 is the recovery factor as given in ref. 7. The velocity V_2 , enthalpy H_2 and pressure P_2 behind the normal shock are computed by the real gas solution of Moeckel (ref. 8). Using these normal shock values, the other required flow conditions are calculated as follows:

$$a_2 = \sqrt{\gamma_2 \left(\frac{P_2}{\rho_2} \right)} \quad (8)$$

$$M_2 = V_2 / a_2 \quad (9)$$

$$\rho_2 = \frac{P_2}{Z_2 R T_2} \quad (10)$$

$$P_{st} = P_2 \left(1 + \frac{\gamma_2 - 1}{2} M_2^2 \right)^{\frac{\gamma_2}{\gamma_2 - 1}} \quad (11)$$

$$\rho_{st} = \rho_2 \left(1 + \frac{\gamma_2 - 1}{2} M_2^2 \right)^{\frac{1}{\gamma_2 - 1}} \quad (12)$$

$$T_{st} = T_2 \left(1 + \frac{\gamma_2 - 1}{2} M_2^2 \right) \quad (13)$$

$$\rho_w = \frac{P_{st}}{Z_w R T_w} \quad (14)$$

The values for T_2 , γ_2 , ρ_2 , μ_w , μ_{ST} and Z are determined from the real gas tables of ref. 6. It may be noted that the Z in equations 10 and 14 is the compressibility factor in the thermal equation of state for air.

The application of the above method to calculate supersonic and hypersonic stagnation point and leading edge heating on flight vehicles is presented in Appendix A.

Constant Entropy Solutions[†]

The method used to calculate transient aerodynamic heating for constant entropy flow is discussed in this section.

Transient Heating Equation

The following equation is used to calculate transient surface temperatures and heat flux.

$$q = (\rho_w C_{p,w} \tau) \dot{T}_w = (h)(H_R - H_W) - \beta T_w^4 + S \quad (15)$$

Equation 15 is the same as equation 2 except that the empirical F factor in equation 2 is omitted. As was the case for stagnation point calculations, to obtain accurate surface temperatures and heat flux the proper value for the heat capacity $(\rho_w C_{p,w} \tau)$ must be used. The only way to significantly vary the heat capacity is to change the skin thickness (τ) . For metallic surfaces the actual skin thickness gives good results for thickness up to 0.1 inches. For metallic thickness greater than 0.1 inches the value for τ given in the previous section should be used, and for thicknesses greater than 0.2 inches, a thermal analysis may be necessary. For surfaces that are insulated with low conductivity insulation (e.g. space shuttle), a material thickness should be used that results in a heat capacity of approximately 0.1 Btu/ft² °R

Laminar Heat Transfer

To solve equation 15 the heat transfer coefficients are calculated by the following relationship:

$$h = (F) \frac{0.332}{\sqrt{\text{Re}_L}} \sqrt{\frac{\rho^* \mu^*}{\rho_L \mu_L}} (Pr_w)^{-0.6} (\rho_L V_L) \quad (16)$$

which reduces to

[†]Although constant entropy flow will only occur on a surface with a sharp leading edge or nose, many aircraft surfaces can be approximated by shapes where constant entropy solutions can be used with good results.

$$h = (F)0.332\sqrt{\frac{\rho^*\mu^*V_L}{x}}(Pr_w)^{-0.6} \quad (17)$$

Equation 16 is based on the Blasius incompressible skin friction formula (ref. 10) and is related to heat transfer by a modified Reynolds analogy by the following formula:

$$ST = RA \frac{C_f}{2} \quad (18)$$

where $(Pr_w)^{-0.6}$ is the modified Reynolds analogy factor and the Stanton number “ST” is given by:

$$ST = \frac{h}{\rho V} \quad (19)$$

and the Blasius skin friction formula is:

$$\frac{C_f}{2} = 0.332(Re_L)^{-1/2} \quad (20)$$

Compressibility effects are accounted for by Eckert’s reference enthalpy method (refs. 11 and 12), and the flow properties are evaluated at the reference enthalpy given by the following equation:

$$H^* = 0.5(H_w + H_L) + 0.22(H_R + H_L) \quad (21)$$

where

$$H_R = H_L + \sqrt{Pr_w} \frac{V_L^2}{2gJ} \quad (22)$$

and

$$H_w = f(T_w, P_L)$$

$$H_L = f(T_L, P_L)$$

$$T^* = f(H^*, P_L)$$

$$\mu^* = f(T^*, P_L)$$

The values of H_w , H_L , T^* and μ^* are obtained from real gas tables. (ref. 6).

The value for ρ^* is calculated from the following equation:

$$\rho^* = \frac{P_L}{Z^* R T^*} \quad (23)$$

where $Z^* = f(T^*, P_L)$ and is obtained from ref.6.

Turbulent Heat Transfer

The turbulent heat transfer coefficient is obtained by solving for the turbulent skin friction coefficient and then relating the skin friction to heat transfer by a modified Reynolds analogy. Two methods are available in the TPATH to calculate turbulent heat transfer. The first is the skin friction theory of van Driest (ref. 13) given by the following equation:

$$\frac{0.242}{A \sqrt{C_f} \sqrt{\frac{H_w}{H_L}}} \left[\sin^{-1} \frac{A - B/2A}{\sqrt{(B/2A)^2 + 1}} + \sin^{-1} \frac{B/2A}{\sqrt{(B/2A)^2 + 1}} \right] - 0.41 - \log(\text{Re}_L C_f) + 0.76 \log \frac{H_w}{H_L} = 0 \quad (24)$$

where

$$A = \sqrt{\frac{\frac{\gamma-1}{2} M_L^2}{H_w/H_L}} \text{ and } B = \frac{1 + \frac{\gamma-1}{2} M_L^2}{H_w/H_L} - 1.0$$

The heat transfer coefficient is then calculated by relating heat transfer to skin friction by equation 18 and using the following modified Reynolds analogy factor:

$$\text{RA} = (\text{Pr}_{w})^{-0.4} \quad (25)$$

The heat transfer coefficient calculated by the van Driest method is then given by the following equation:

$$h = F \frac{C_f \rho_L V_L}{2(\text{Pr}_{w})^{0.4}} \quad (26)$$

The second method for calculating turbulent heat transfer in the TPATH program uses the following incompressible skin friction equation:

$$\frac{C_f}{2} = \frac{0.185}{(\log \text{Re}_L)^{2.584}} \quad (27)$$

This equation is transformed to the compressible plane by Eckert's reference enthalpy method (ref. 11) resulting in the following equation for compressible skin friction:

$$\frac{C_f}{2} = \frac{0.185}{(\log \text{Re}^*)^{2.584}} \left(\frac{\rho^*}{\rho_\infty} \right) \quad (28)$$

where the density and viscosity in the Reynolds number are evaluated at the reference enthalpy (eq. 21), and the recovery enthalpy (H_R) is computed from the following equation:

$$H_R = H_L + (Pr_w)^{1/3} V_L^2 / 2gJ \quad (29)$$

Equation 28 is then related to the heat transfer coefficient by a modified Reynolds analogy (eqs. 18, 19 and 25) resulting in the following equation:

$$h = F \frac{0.185}{(\log \text{Re}^*)^{2.584}} (Pr_w)^{-0.4} (\rho_L^* V_L) \quad (30)$$

The enthalpy H_w and the Prandtl number Pr_w are functions of temperature and boundary-layer edge static pressure and are obtained from real gas tables. (ref. 6).

The F factors in equation 17, 26, and 30 are usually used to correct two-dimensional heat transfer coefficient to conical flow values. The transformation factors are 1.73 and 1.15 for laminar and turbulent flow respectively. (ref. 11).

The methods used to calculate the local flow values required to solve the above equations and the application of the above methods to calculated supersonic and hypersonic laminar and turbulent heat transfer on flight vehicles are discussed in Appendix B. It should be noted that real gas properties are used in all solutions. (ref. 6).

Variable Entropy Solutions

The method used to calculate transient aerodynamic heating for variable entropy flow is presented in this section.

Transient Heating

The transient equation for variable entropy is

$$q = \left(\rho_w C p_w \tau \right) \dot{T}_w = h(H_R - H_w) - \beta T_w^4 + S \quad (31)$$

The equations used to calculate the heat transfer coefficients for constant entropy flow could also be used for variable entropy flow[‡] if the local flow conditions at the edge of the boundary layer are known. The equations and procedure for determining the boundary layer edge condition and subsequently the heat transfer coefficient for laminar and turbulent flow, under variable entropy conditions, is described below.

Laminar Heat Transfer

To calculate heat transfer coefficients for variable entropy flow, it is more convenient to define the heat transfer coefficient in terms of momentum thickness θ instead of flow distance x . In terms of momentum thickness the heat transfer coefficient is given by the following equation:

$$h = 0.22(R\theta, L)^{-1} \left(\frac{\mu^*}{\mu_L} \right) (Pr_w)^{-0.6} (\rho_L V_L) \quad (32)$$

This equation is obtained by relating the Blasius incompressible skin friction equation (ref. 10) to heat transfer by a modified Reynolds analogy factor and accounting for compressible effects by Eckert's reference enthalpy method (refs. 11 and 12). For Eckert's method, the flow properties are evaluated at the reference enthalpy given by the following equation

$$H^* = 0.5(H_w + H_L) + 0.22(H_R - H_L) \quad (33)$$

The momentum thickness “ θ ” is calculated for axisymmetric flow by (ref. 13).

$$\theta = 0.664 \frac{\left[\int_0^x \rho^* \mu^* V_L r^2 dx \right]^{1/2}}{\rho^* V_L r} \quad (34)$$

and for two-dimensional flow by

$$\theta = 0.664 \frac{\left[\int_0^x \rho^* \mu^* V_L dx \right]^{1/2}}{\rho^* V_L} \quad (35)$$

For constant pressure surfaces, equation 35 reduces to the well-known flat plate equation

$$\theta = 0.664 \sqrt{\frac{\mu^* x}{\rho^* V_L}} \quad (36)$$

[‡]All surfaces with a blunt leading edge or blunt nose will have variable entropy flow.

Equation 36 may also be used for two-dimensional surfaces with small pressure gradients with satisfactory results. Equations 34 and 35 provide a technique to include the effect of geometry and variable edge conditions about a blunt body on the laminar momentum thickness calculations.

Turbulent Heat Transfer

The turbulent heat transfer is also computed by using a skin friction based on the momentum thickness and relating the skin friction to heat transfer by the following modified Reynolds analogy factor:

$$RA = (Pr_w)^{-0.4} \quad (37)$$

The skin friction equation used for turbulent flow is

$$\frac{C_f}{2} = c_1(R\theta_L)^{-m} \quad (38)$$

which for an assumed 1/7th velocity profile results in the well known Blasius incompressible skin friction relationship (ref. 10) of

$$\frac{C_f}{2} = 0.0128(R\theta_L)^{-1/4} \quad (39)$$

It is known that the velocity profile exponent for turbulent flow varies with Reynolds number. Therefore, a relationship between Reynolds number and the velocity profile exponent is required to obtain good results over a wide range of Reynolds numbers. Reference 14 gives the following relationship for axisymmetrical flow

$$N = 12.67 - 6.5\log(R\theta_L) + 1.21(\log R\theta_L)^2 \quad (40)$$

For two-dimensional flow the following equation was determined from measured data of (ref. 15).

$$N = 14.92 - 6.5\log(R\theta_L) + 1.21(\log R\theta_L)^2 \quad (41)$$

From equations 37 and 38 and Eckert's reference enthalpy (equation 33), to account for compressibility, the following equation for the turbulent heat transfer coefficient is obtained

$$h = c_1(R\theta_L)^{-m} \left(\frac{\mu^*}{\mu_L} \right)^m \left(\frac{\rho^*}{\rho_L} \right)^{(1-m)} (Pr_w)^{-0.4} (\rho_L V_L) \quad (42)$$

The momentum thickness is calculated for axisymmetric flow by

$$\theta = \frac{\left[c_2 \int_0^x \rho^* V_L (\mu^*)^m r^{c_3} dx \right]^{c_4}}{\rho^* V_L r} \quad (43)$$

and for two-dimensional flow by

$$\theta = \frac{\left[c_2 \int_0^x \rho^* V_L (\mu^*)^m dx \right]^{c_4}}{\rho^* V_L} \quad (44)$$

which for constant pressure surfaces reduces to the flat plate equation

$$\theta = \frac{\left[c_2 V_L \rho^* (\mu^*)^m x \right]^{c_4}}{\rho^* V_L} \quad (45)$$

The relations for the exponents and coefficients in equation 42 through 45 are given as (ref. 14)

$$m = \frac{2}{N+1} \quad (46)$$

$$c_1 = \left(\frac{1}{c_5} \right)^{\frac{2N}{(N+1)}} \left[\frac{N}{(N+1)(N+2)} \right]^m \quad (47)$$

$$c_2 = (1+m)c_1 \quad (48)$$

$$c_3 = 1+m \quad (49)$$

$$c_4 = \frac{1}{c_3} \quad (50)$$

$$c_5 = 2.243 + 0.93N \quad (51)$$

The boundary layer thicknesses are then determined by the following equation

$$\frac{\delta}{\theta} = 5.55 \quad (52)$$

For laminar flow on bodies of revolution (ref. 14), or:

$$\frac{\delta}{\theta} = 7.50 \quad (53)$$

For laminar flow on wings (ref. 10), or:

$$\frac{\delta}{\theta} = N + 1 + \left[\left(\frac{N + 2 \frac{H_w}{H_R}}{N} + 1 \right) \times \left(1 + 1.29 (Pr_w)^{0.33} \frac{V_L^2}{2gJH_L} \right) \right] \quad (54)$$

For turbulent flow on bodies of revolution (ref. 14) and

$$\frac{\delta}{\theta} = N + 1 + \left[\left(\frac{N + 2 \frac{H_w}{H_R}}{N} + 1.4 \right) \times \left(1 + 1.29 (Pr_w)^{0.33} \frac{V_L^2}{2gJH_L} \right) \right] \quad (55)$$

for turbulent flow on wings. Equation 55 was obtained based on results of reference 15.

The values of H_w , H_L and Pr_w are determined from real gas tables obtained from reference 6.

To solve the above for variable entropy flow, an inviscid CFD solution is assumed to be known[§]. Then, by means of an iterative process, the momentum thickness, equations 34, 35, 43, and 44, the reference enthalpy equation 33, and corresponding ratios of boundary layer thickness to momentum thickness (eqs. 52 through 55) are used to determine the local flow at the edge of the boundary layer. This procedure accounts for variable entropy effects by locally moving out in the inviscid flow field at a distance equal to the boundary layer thickness, δ . These results must then be coupled with the transient heating equation (eq. 31) to solve for the transient surface temperatures and heat flux. This method for accounting for variable entropy flow has been shown by Zoby (refs. 14 and 16) to produce aerodynamic heating that is in good agreement with viscous CFD solutions and with measured data.

The procedure used in the TPATH program to calculate the local flow values required to solve the above equation are presented in Appendix C.

Boundary Layer Transition Criteria

The transition from laminar to turbulent flow has been the subject of investigation for over 100 years. However, the prediction of boundary layer transition is still more of an art than a science. Two of the primary parameters that affect boundary layer transition are the local Reynolds number and local Mach number. The TPATH program uses the following equation that incorporates these parameters to predict transition:

[§]The inviscid CFD solution can also be used for constant entropy flow.

$$\log \text{Re}_{,L} > \left[\log \text{Re}_{,t} + C_M(M_L) \right] \quad (56)$$

Based on this equation, if the log of the local Reynolds number ($\text{Re}_{,L}$) at a given point in the trajectory, is greater than the log of the local transition Reynolds number plus the transition Mach number coefficient (C_M) times the local Mach number, then the TPATH calculates values for turbulent flow. If the log of the Reynolds number is equal to or less than this value, then laminar flow values are calculated. The user must input the log of the transition Reynolds number and the transition Mach number coefficient. The following table lists the transition Reynolds number and Mach number coefficients recommended:

Recommended transition Reynolds number and Mach number coefficients.		
	$\log \text{Re}_{,t}$	C_M
Fuselage	5.5	0.2
Wing – no sweep	5.5	0.2
Wing – with sweep	5.5	0.1

Of course these recommendations are subject to change if specific information is available that might cause premature transition such as any or all of the following: surface roughness, shock interaction, or flow field contamination.

RESULTS AND DISCUSSION

The heat transfer theory described in the preceding sections has been used to predict temperatures and heat flux in support of numerous high-speed flight programs. Some of these programs have produced measured data that was compared to calculated values. Comparisons between measured data and predicted values for the X-15 research airplane, space shuttle orbiter and the YF-12 are presented below.

X-15 Airplane

Figures 1 through 7 present comparisons of calculated values with temperatures or heat transfer coefficients measured on the X-15 airplane. Figure 1 shows a comparison of calculated and measured temperatures on the wing leading edge for a flight to a Mach number 6.0 (ref. 17). As can be seen the agreement is excellent. Figure 2 shows comparisons of temperatures measured on the wing midsemispan (ref. 17). The comparisons are made at the 4-, 10-, 20- and 46-percent chord. Calculated temperatures are shown for laminar and turbulent flow. At the 4 percent chord the laminar calculated values are in good agreement with the measured data. The boundary-layer flow was obviously laminar at this location. At the 20- and 46-percent chord the measured data are in good agreement with the calculated temperatures for turbulent flow. As can be seen at the 10-percent chord, the temperatures predicted assuming laminar flow are slightly lower than the measured data. This indicates that the boundary layer at the 10-percent chord is mostly laminar flow with some transitional flow. Figure 3 shows comparisons of calculated and

measured heat transfer coefficients (ref. 18). The data were measured during two flights. In one flight the boundary layer was turbulent from just aft of the leading edge to the trailing edge. In the other flight, the boundary layer was laminar for the first foot of the midsemispan and transitioned to turbulent flow between 1 and 1.4 ft. As shown, the calculated values are in good agreement with both the laminar and turbulent data. Figure 4 shows a comparison of measured and calculated temperatures for a low altitude flight and a high altitude flight (ref. 18). Both flights obtained a maximum Mach number of 5.0. The data were measured on the wing midsemispan 1.4 ft aft of the leading edge. For the low altitude flight the agreement between measured and calculated temperatures is good. For the high altitude flight the agreement is also good if the time of boundary-layer transition is known. Figure 5 (ref. 17) shows a comparison of measured and calculated temperatures on the lower fuselage at station 72.5 for a flight to a Mach number of 6.0. Also shown in figure 5 is a time history of the calculated local surface static pressure with comparison to flight measured data. As can be seen, the measured temperatures and static pressures are in good agreement with calculated values. Figure 6 (ref. 18) shows comparisons of measured and calculated temperatures on the lower fuselage centerline and the lower speed brake. The measured data were obtained during a Mach 5.0 flight. As shown, the calculated temperatures for the fuselage are slightly higher than the measured values at the maximum temperature, however, the overall agreement is good. The calculated temperatures for the speed brake are in good agreement with measured data for the heating portion of the flight but somewhat over predict the flight data during cool down. This overprediction is probably the result of internal conduction that is not accounted for in the TPATH program. The overall agreement is considered good. Figure 7 (ref. 19) shows a comparison of measured and calculated Stanton numbers for the upper vertical tail. The data were obtained at a free stream Mach number of 5.25. The calculated Stanton numbers are in excellent agreement with the measured data when the flow is fully turbulent.

Space Shuttle

Temperatures measured on the lower wing of the space shuttle (ref. 20) are compared in figure 8 with values calculated using the TPATH program. The calculated temperatures are in good agreement with the measured data except just before touchdown when the calculations overpredict the measured data. This discrepancy is caused by internal cooling resulting from atmospheric air entering wing bays to equalize pressure (ref. 21). It may be noted that transition from laminar to turbulent flow occurred at approximately 1150 sec. Temperatures measured on the lower fuselage (ref. 22) are compared with calculated temperatures in figure 9. The calculated values slightly underpredict the measured data at the maximum temperatures. However, the overall agreement is good. The overprediction just before touchdown due to internal cooling is again evident.

YF-12 Airplane

Figure 10 shows comparisons between calculated and measured temperatures obtained on the lower wing at three locations. The data were obtained during a flight to a Mach number of 3.0, and are taken from reference 23. The calculated temperatures for $x = 0.8$ ft are in excellent agreement with the measured data. The calculated temperatures for $x = 14.0$ and 39 ft slightly over predict the measured data. These overpredictions are due to conduction losses to the large spars that are close to these locations. These conduction losses are not accounted for in the TPATH program. The overall agreement is considered to be good since the overprediction is expected in areas near substructure and the temperatures are close enough that the effect on the heat transfer coefficient is negligible. Figure 11 shows a comparison of measured and calculated Stanton numbers. The data were measured on a hollow

cylinder (ref. 15) during a YF-12 boundary-layer experiment. The data were obtained at steady state flight conditions at a free stream Mach number of 3.0. The measured data are compared with values predicted by the theory of van Driest. The theory of van Driest is one of the two turbulent theories used to calculate transient aerodynamic heating in the TPATH program. As shown in Figure 11, the agreement between measurements and theory is excellent. It may be noted that fully developed turbulent flow occurred approximately at a Reynolds number of 1.2 million.

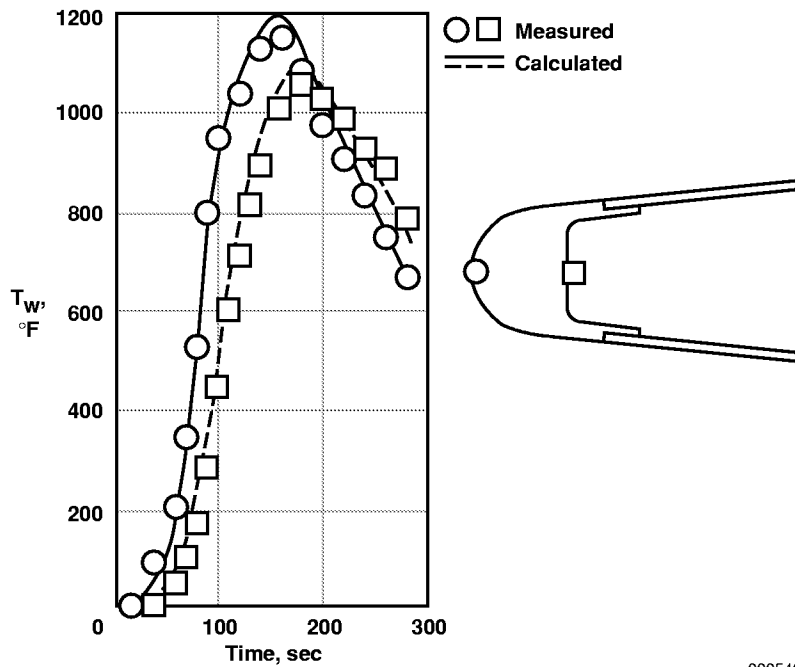
CONCLUDING REMARKS

An aerodynamic heating program called TPATH used at the NASA Dryden Flight Research Center to calculate transient surface temperatures and heating rates has been described. The semi-empirical aerodynamic heating theories used in the program have been presented in detail and the procedures used for calculating the local flow at the edge of the boundary layer for both constant and variable entropy flow has been presented. In addition, boundary-layer transition criteria were presented. The application of these approximate methods to calculate supersonic and hypersonic laminar and turbulent heat transfer on flight vehicles has been described.

Transient surface temperatures and heating rates predicted by this program were compared to flight measured data obtained on the X-15 research vehicle, the YF-12 airplane and the Space Shuttle orbiter. These comparisons show that the values predicted using the TPATH program are in good agreement with measured surface temperatures and measure heat transfer coefficients.

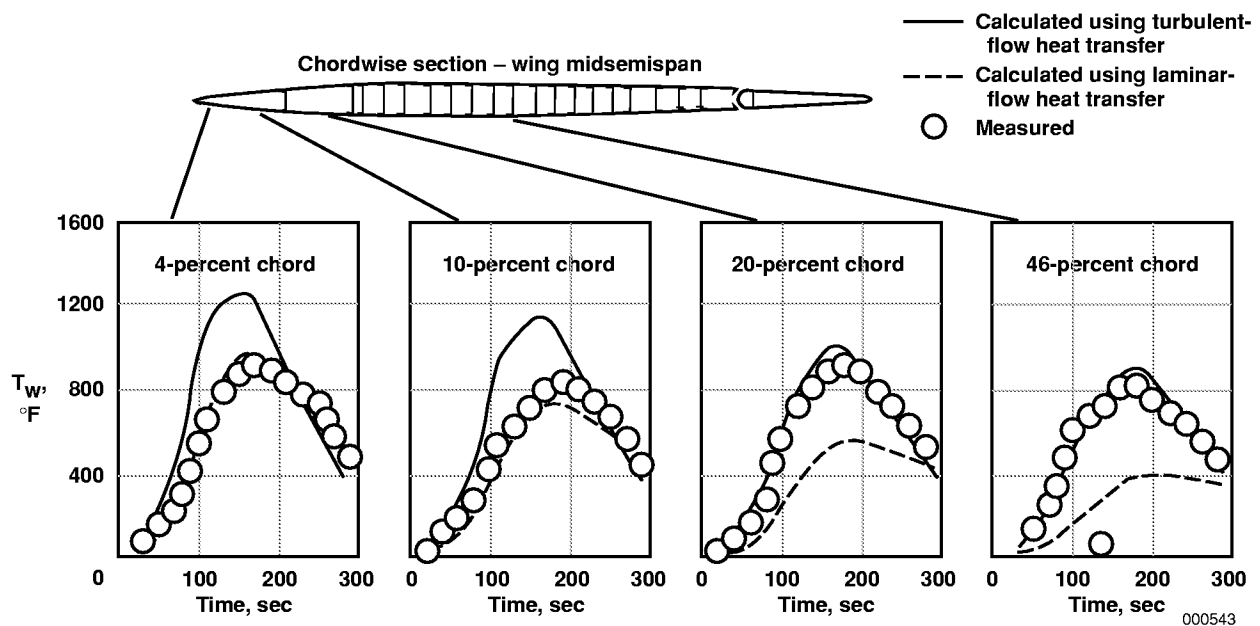
*Dryden Flight Research Center
National Aeronautics and Space Administration
Edwards, California, August 24, 2000*

FIGURES



000542

Figure 1. Comparison of measured and calculated temperatures on the leading edge of the X-15 airplane. $M_{\infty} = 6.0$.



000543

Figure 2. Comparison of measured and calculated surface temperatures on the wing midsemispan of the X-15 airplane. $M_{\infty} = 6.0$.

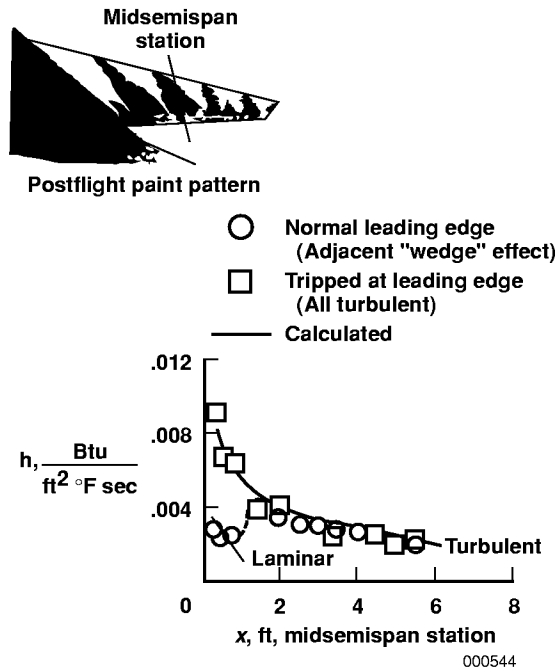


Figure 3. Measured and calculated heat transfer on the X-15 wing. $M_\infty = 4.4$.

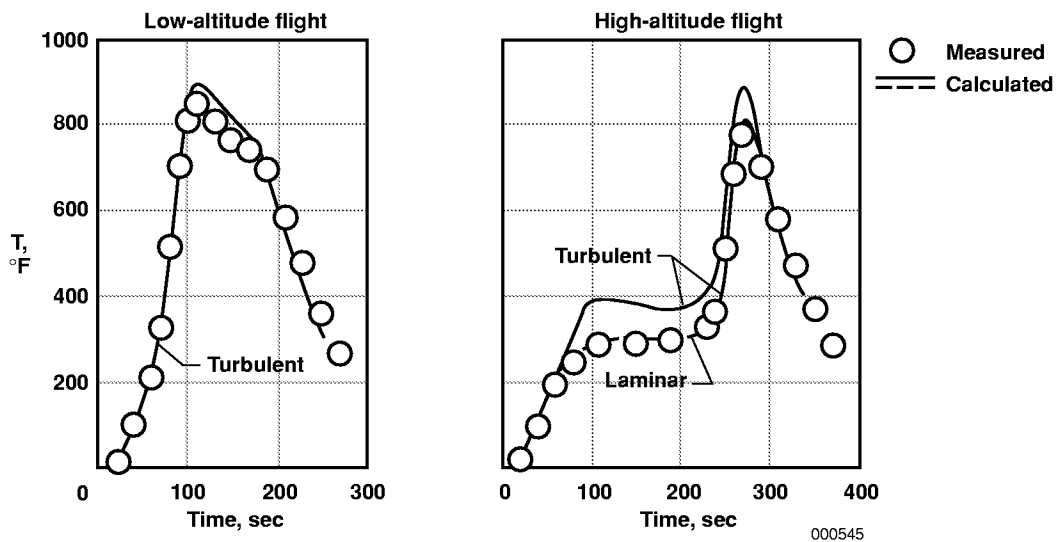


Figure 4. Comparison of measured and calculated surface temperatures on the X-15 wing lower midsemispan. $M_\infty = 5.0$, $x = 1.4$ ft.

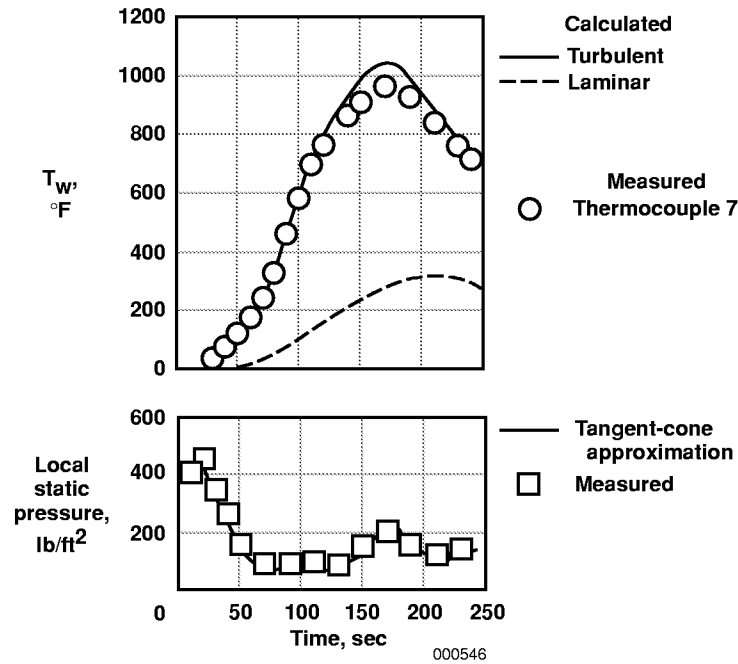


Figure 5. Comparison of measured and calculated temperature and surface static pressure for fuselage bottom centerline at fuselage station 72.5. $M_{\infty} = 6.0$.

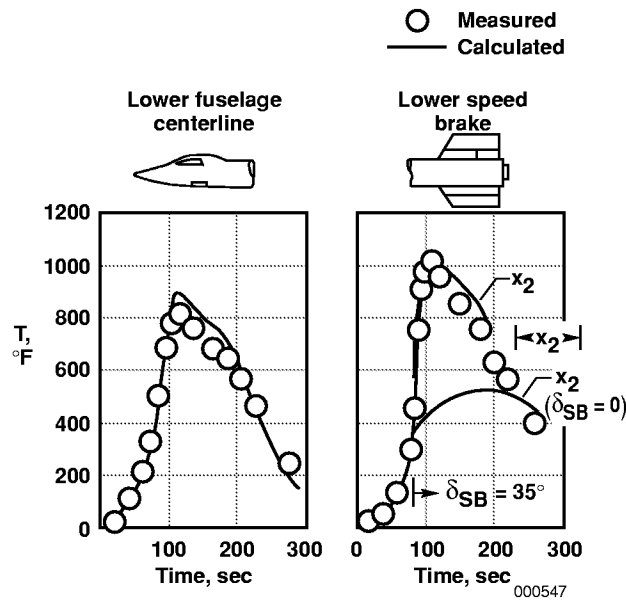


Figure 6. Comparison of measured and calculated surface temperatures on the fuselage and speed brake of the X-15 airplane. $M_{\infty} = 5.0$.

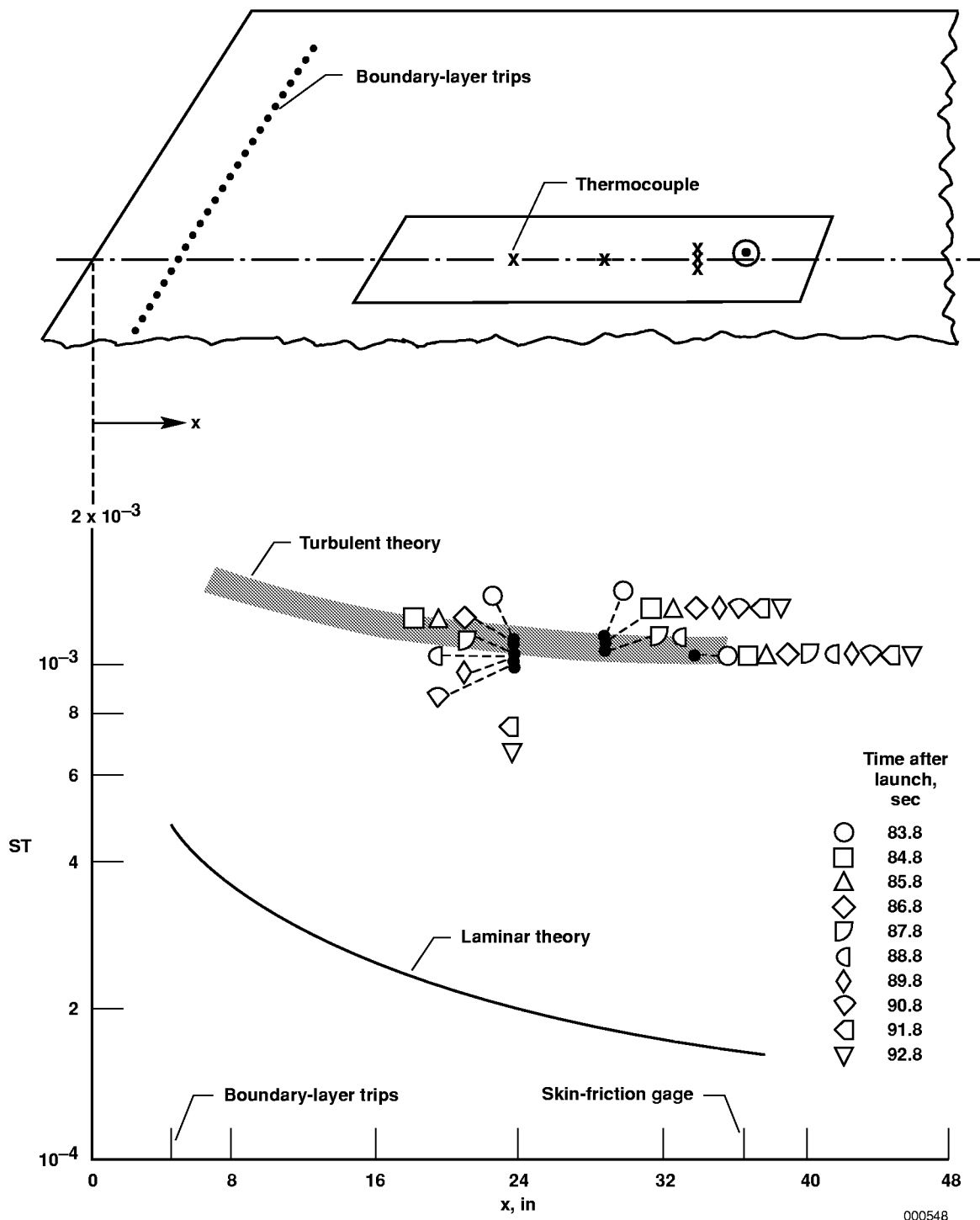


Figure 7. Comparison of measured and calculated heat transfer on the vertical tail of the X-15 airplane. $M_{\infty} = 5.25$.

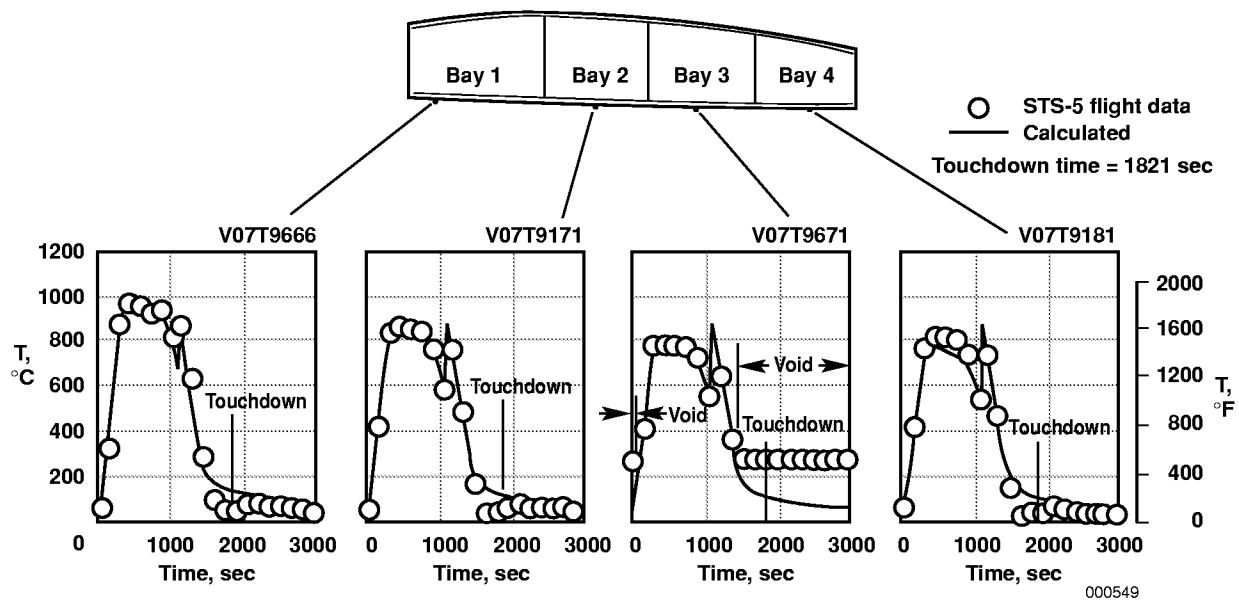


Figure 8. Comparison of measured and calculated surface temperatures on the wing of the Space Shuttle Orbiter.

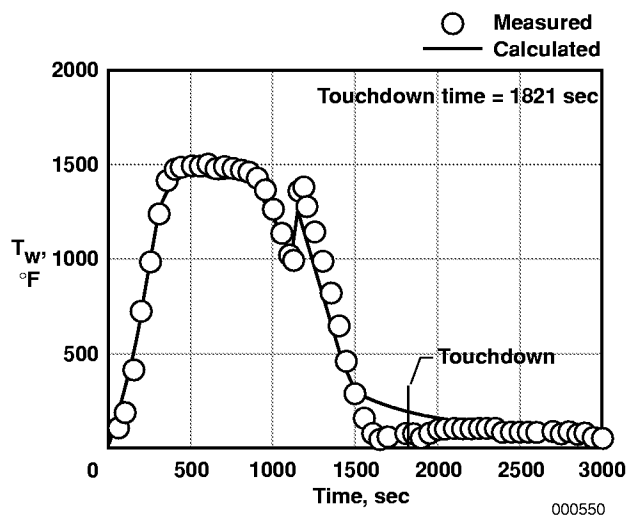


Figure 9. Comparison of measured and calculated surface temperatures on the lower fuselage centerline at fuselage station 877 of the Space Shuttle.

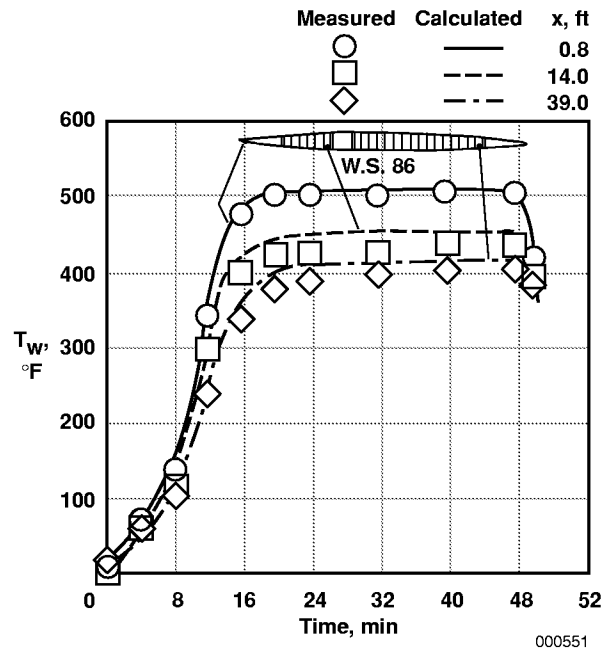


Figure 10. Comparison of flight measured and calculated surface temperatures on the lower wing of the YF-12 airplane. $M_{\infty} = 3.0$.

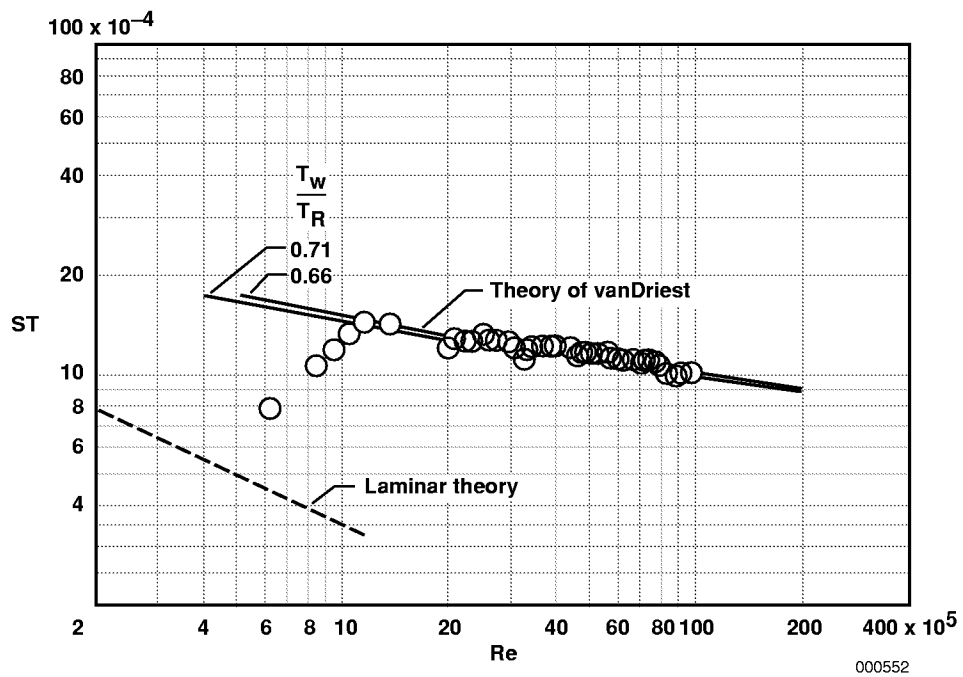


Figure 11. Comparison of measured and calculated heat transfer. $M_{\infty} = 3.0$.

APPENDIX A

Calculating Stagnation Point and Leading Edge Heating for High-Speed Vehicles

The calculation of stagnation point heating using the TPATH program (equations 1 through 9) is straightforward. The method, described in the stagnation point section, is shown in this report to produce excellent results. However, this program does not have a direct means of computing the circumferential heating on spherical or cylindrical leading edges. Equations are available to make these calculations (ref. 5) and these equations are scheduled to be incorporated in the TPATH program.

In lieu of the exact equations, the following methodology is used to compute circumferential heat transfer on cylinders and spheres. This method can be used for any leading edge or nose of a vehicle that can be approximated by a cylinder or sphere. Figures A-1 and A-2 show curves of heat transfer compared with circumferential angle (θ_s) for a sphere and cylinder. These curves are based on the Lees theory (ref. 24). Although figures A-1 and A-2 show heating values from $\theta_s = 0$ deg to $\theta_s = 90$ deg, it is well known that the values for θ_s greater than 70 deg are questionable. Therefore, these curves should only be used for values of θ_s from 0 to 70 deg. This is not a restriction since most if not all leading edges end before $\theta_s = 70$ deg. In other words, the cylindrical portion of a leading edge ends by $\theta_s = 70$ deg and the wing or fuselage surface begins. Therefore, to calculate the heating rate for say $\theta_s = 20, 40$ and 60 deg, go to one of these curves, choose the ratio of q/q_0 and use this value as the F factor in equation 1 or 2 to calculate the heating temperatures for these locations.

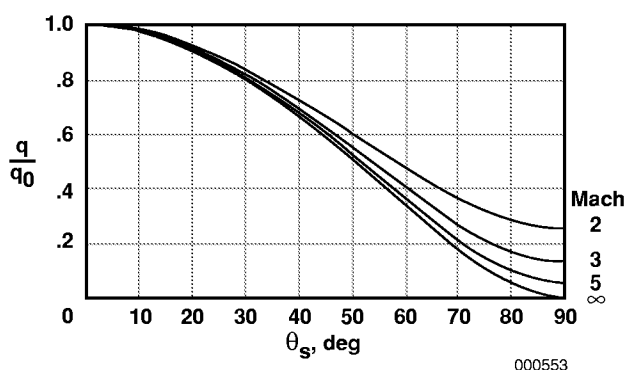


Figure A-1. Heating distribution on a hemisphere.

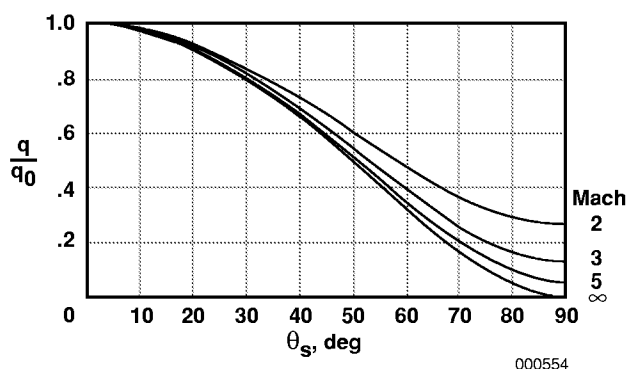


Figure A-2. Heating distribution on a cylinder.

APPENDIX B

Calculating Local Flow for Laminar and Turbulent Heat Transfer on High-Speed Aircraft

The approximate methods in the TPATH program used to calculate heat transfer and temperatures have been shown (ref. 15 through 22) to predict values that are in good agreement with measured data when the proper values for the local flow at the edge of the boundary layer are used. Since the ability of the TPATH program to calculate local flow values is limited, engineering judgment and experience must be used to calculate the local flow values that will provide good heating results.

The TPATH program has the ability to use free stream conditions for local flow or to calculate local flow by means of a real gas solution for the oblique shock theory (ref. 6), Prandtl-Meyer expansion theory (ref. 9) or tangent cone theory (ref. 25). It should be noted that all shock solutions used in the TPATH program are real gas shock solutions. Ideal gas solutions are not used because they will produce inaccurate results for high-speed flow. With these theories, the local flow values can be obtained for flat plates, wedges, cones or any surface where two-dimensional expansion can be assumed. Although aircraft are not made of flat plates, wedges, or cones, it is fortunate that many aircraft surfaces can be approximated by flat plates, wedges or cones. Specific recommendations for calculating the local flow properties required by the heating equation are presented below. These recommendations are based on many years of experience and have been shown to predict accurate heating rates and/or surface temperatures (See Results and Discussion Section) for the YF-12 airplane, the X-15 airplane and the space shuttle orbiter.

Wing

The heating rates for the leading edge are calculated by the procedure explained in Appendix A. For the wing surface aft of the leading edge the following two methods are used.

Method 1

The flow conditions in front of the wing are assumed to be free stream. This is usually not true since the fuselage forebody will change the flow conditions in front of the wing. However, for most forebodies except those with large blunt noses this assumption is adequate. Assume a wedge half-angle that is equal to the angle between the wing center line and a line that is tangent to the leading edge at the point where the cylindrical leading edge ends and the wing skin begins. See figure B-1 below.

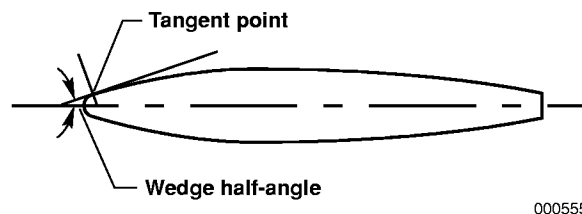


Figure B-1. Wing cross section

Using this wedge half-angle, the local flow condition at the tangent point is calculated by oblique shock theory with sweep angle neglected (e.g. sweep angle equal to zero). The local flow aft of the oblique shock is then used as inputs to the Prandtl-Meyer expansion theory to calculate the flow over the entire wing.

Method 2

For this method it is assumed that the local flow conditions in front of the wing shock are known (e. g. from an inviscid CFD solution for the fuselage forebody). To calculate the flow at the wing surface aft of the leading edge skin tangent point, the following procedure is used:

The modified Newtonian theory, as given by the following equation:

$$\left[P_L = P_{st} \cos^2 \theta_s + P_1 \sin^2 \theta_s \right] \quad (B-1)$$

is used to calculate the surface static pressure around the cylindrical leading edge to the tangent point. The modified Newtonian theory has been shown (ref. 5) to predict static pressure that is in good agreement with measured data. Then make a swept oblique shock calculation using a wedge half-angle that results in a calculated surface static pressure at the tangent point that is equal to the pressure calculated by the modified Newtonian theory at that point. Then use the results from the swept oblique shock solution together with the Prandtl-Meyer expansion theory to calculate the local flow on the upper and lower wing surfaces.

Fuselage

The heat rates and temperatures for the nose of the fuselage are calculated using the procedure described in Appendix A. The local flow conditions on the lower fuselage centerline $\phi = 0$ deg is calculated by the tangent cone method (ref. 25). This method assumes that the local surface static pressure is equivalent to the pressure on a cone with a semi-vertex angle equal to the angle between the tangent to the surface and the direction of the flow. This method is shown in ref. 25 and figure 5 of this report to predict values that are in good agreement with the measured surface static pressures. The total pressure calculated behind the conical shock for the given semi-vertex angle is then used together with the static pressure to calculate the other local flow values (ref. 9), or the user can input a value for the total pressure. If the nose is not too blunt[†], such as the YF-12 or X-15 airplanes, the total pressure produced by the conical shock is satisfactory. If the nose is very blunt such as the space shuttle, a total pressure that is about half way between the conical shock value and the normal shock will produce satisfactory results. The above procedure provides a means for varying the total pressure as one moves aft on the fuselage and can be used to approximate local flow values for variable entropy calculation.

For circumferential local flow values, the local static pressures are calculated by the method given in (ref. 26). The total pressure is input by the user and depends on circumferential locations. See figure B-2. For $\phi = 90$ deg a total pressure equal to that behind the conical shock is usually a good approximation and for $\phi = 180$ deg (top centerline) a total pressure between the conical shock value and the free stream value is used depending on the angle of attack.[#] the conical shock value is appropriate,

[†]The definition of what is and what is not too blunt depends not only on the nose radius, but also on the overall shape of the fuselage forebody. As an initial guide, it may be assumed that a radius of 6.0 inches or less is not too blunt.

[#]For the purpose of this discussion, an angle of attack from 0–10 degrees is low.

and for high angles of attack the free stream total pressure will produce satisfactory results. With the local static and total pressures known, the other local flow conditions are calculated using the standard compressible equation (ref. 9).

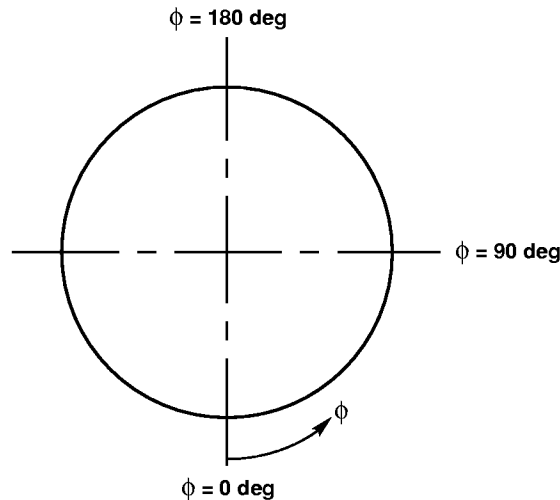


Figure B-2. Fuselage cross section.

Once the local flow values are determined, they are input into equations 12, 20, or 24 to calculate the heat transfer coefficient, and the heat transfer coefficient is then used in equation 10 to calculate the transient surface temperatures and heating rates. It should be noted that for conical flow the F factor in equations 12, 20, and 24 should be 1.15 for turbulent flow and 1.73 for laminar flow.

APPENDIX C

Local Flow Calculation for Variable Entropy Solutions

The heating equations necessary to calculate transient aerodynamic heating and surface temperature for variable entropy flow (e.g. blunt bodies) have been presented in the Variable Entropy Solutions section (eqs. 25 through 48). In order to solve these equations the local flow values must be determined. The first choice for predicting the local flow for blunt bodies of an arbitrary cross section is a general inviscid CFD solution. A general inviscid CFD solution for wing/body combination of an arbitrary cross section is being developed under a grant to UCLA and will be incorporated into the TPATH when completed. In the meantime, one must resort to an approximate method to calculate the local flow values required to obtain variable entropy solutions. The following methods are recommended until the inviscid CFD solution is available:

Wing

For wings with relative small leading edge bluntness^{**} (e.g. X-15 and YF-12) the methods given in Appendix B can be used with satisfactory results. For wings with large blunt leading edges (e.g. space shuttle) the tangent wedge method should be used. This method uses the angle between the tangent to the surface and the direction of flow as a wedge half-angle. Using this wedge half-angle, the local flow conditions at the tangent point are calculated by oblique shock theory. A new wedge half-angle is determined for each point on the wing where calculations are to be made. This method provides a means to vary the entropy along the wing surface.

Fuselage

The method presented in Appendix B can be used to approximate the local flow values for variable entropy solutions.

^{**}The definition of what may be considered small leading edge bluntness depends not only on the radius of the leading edge, but also the shape of the wing aft of the leading edge. As an initial guide, a radius of 1 inch or less is assumed to be small leading edge bluntness.

REFERENCES

1. Gnoffo, P. A., K. J. Weilmuenster, H. H. Hamilton II, D. R. Olynick, and E. Venkatapathy, "Computational Aerothermodynamic Design Issues for Hypersonic Vehicles, *Journal of Spacecraft and Rockets*, vol. 36, no. 1, January–February 1999, pp. 21–43.
2. Cheatwood, F. McNeil and Peter A. Gnoffo, *Users Manual for the Langley Aerothermodynamic Upwind Relaxation Algorithm (LAURA)*, NASA TM-4674, April 1996.
3. Quinn, Robert D. and Leslie Gong, *Real-Time Aerodynamic Heating and Surface Temperature Calculations for Hypersonic Flight Simulation*, NASA TM-4222, August 1990.
4. Fay, J. A. and F. R. Riddell, "Theory of Stagnation Point Heat Transfer in Dissociated Air," *Journal of the Aeronautical Sciences*, vol. 25, no. 2, February 1958, pp. 73–85, 121.
5. Beckwith, Ivan E. and James J. Gallagher, *Local Heat Transfer and Recovery Temperatures on a Yawed Cylinder at a Mach Number of 4.15 and High Reynolds Numbers*, NASA TR R-104, 1961.
6. Hansen, C. Frederick, *Approximations for the Thermodynamic and Transport Properties of High-Temperature Air*, NASA TR R-50, 1959.
7. Reshotko, Eli and Ivan E. Beckwith, *Compressible Laminar Boundary Layer Over a Yawed Infinite Cylinder with Heat Transfer and Arbitrary Prandtl Number*, NACA Report 1379, 1958.
8. Moeckel, W. E., *Oblique-Shock Relations at Hypersonic Speeds for Air in Chemical Equilibrium*, NACA TN-3895, January 1957.
9. Ames Research Staff, *Equations, Tables, and Charts for Compressible Flow*, NACA Report 1135, 1953.
10. Schlichting, Hermann, *Boundary Layer Theory*, 4th Ed., McGraw-Hill, New York, 1960.
11. Eckert, Ernest R. G., *Survey on Heat Transfer at High Speeds*, Wright-Air Development Center Technical Report 54-70, April 1954.
12. Eckert, Ernest R. G., *Survey of Boundary Layer Heat Transfer at High Velocities and High Temperatures*, Wright-Air Development Center Technical Report 59-624, April 1960.
13. van Driest, E. R., "The Problem of Aerodynamic Heating," *Aeronautical Engineering Review*, vol. 15, no. 10, October 1956, pp. 26–41.
14. Zoby, E. V., J. N. Moss, and K. Sutton, "Approximate Convective-Heating Equations for Hypersonic Flow," *Journal of Spacecraft and Rockets*, vol. 18, no. 1, January 1981, pp. 64–70.
15. Quinn, Robert D. and Leslie Gong, *In-Flight Boundary-Layer Measurements on a Hollow Cylinder at a Mach Number of 3.0*, NASA TP-1764, November 1980.
16. Zoby, E. V., "Comparisons of Free-Flight Experimental and Predicted Heating Rates for the Space Shuttle," AIAA Paper No. 82-0002, January 1982.

17. Watts, Joe D. and Ronald P. Banas, *X-15 Structural Temperature Measurements and Calculations for Flights to Maximum Mach Numbers of Approximately 4, 5, and 6*, NASA TM X-883, August 1963.
18. Banner, Richard D., Albert E. Kuhl, and Robert D. Quinn, *Preliminary Results of Aerodynamic Studies on the X-15 Airplane*, NASA TM X-638, March 1962.
19. Quinn, Robert D. and Frank V. Olinger, *Flight-Measured Heat Transfer and Skin Friction at a Mach Number of 5.25 and at Low Wall Temperatures*, NASA TM X-1921, November 1969.
20. Ko, William L., Robert D. Quinn, and Leslie Gong, *Finite-Element Reentry Heat-Transfer Analysis of Space Shuttle Orbiter*, NASA TP-2657, December 1986.
21. Ko, William L., Robert D. Quinn, and Leslie Gong, *Effects of Forced and Free Convections on Structural Temperatures of Space Shuttle Orbiter During Reentry Flight*, NASA TM-86800, October 1986. Revised June 1987.
22. Gong, Leslie, William L. Ko, Robert D. Quinn, and Lance Richards, *Comparison of Flight-Measured and Calculated Temperatures on the Space Shuttle Orbiter*, NASA TM-88278, November 1987.
23. Quinn, Robert D. and Frank V. Olinger, "Flight Temperatures and Thermal Simulation Requirements," *NASA YF-12 Flight Loads Program*, NASA TM X-3061, May 1974, pp. 145–183.
24. Lees, Lester, "Laminar Heat Transfer Over Blunt-Nosed Bodies at Hypersonic Flight Speeds," *Jet Propulsion*, vol. 26, no. 4, April 1956, pp. 259–269, 274.
25. Palitz, Murray, *Measured and Calculated Flow Conditions on the Forward Fuselage of the X-15 Airplane and Model at Mach Numbers from 3.0 to 8.0*, NASA TN D-3447, June 1966.
26. Amick, James L., *Pressure Measurements on Sharp and Blunt 5°- and 15°-Half-Angle Cones at Mach Number 3.86 and Angles of Attack to 100°*. NASA TN D-753, February 1961.

REPORT DOCUMENTATION PAGE			Form Approved OMB No. 0704-0188	
<small>Public reporting burden for this collection of information is estimated to average 1 hour per response, including the time for reviewing instructions, searching existing data sources, gathering and maintaining the data needed, and completing and reviewing the collection of information. Send comments regarding this burden estimate or any other aspect of this collection of information, including suggestions for reducing this burden, to Washington Headquarters Services, Directorate for Information Operations and Reports, 1215 Jefferson Davis Highway, Suite 1204, Arlington, VA 22202-4302, and to the Office of Management and Budget, Paperwork Reduction Project (0704-0188), Washington, DC 20503.</small>				
1. AGENCY USE ONLY (Leave blank)		2. REPORT DATE December 2000		3. REPORT TYPE AND DATES COVERED Technical Publication
4. TITLE AND SUBTITLE A Method for Calculating Transient Surface Temperatures and Surface Heating Rates for High-Speed Aircraft				5. FUNDING NUMBERS WU 529-35-34-E8-RR-00-000
6. AUTHOR(S) Robert D. Quinn and Leslie Gong				
7. PERFORMING ORGANIZATION NAME(S) AND ADDRESS(ES) NASA Dryden Flight Research Center P.O. Box 273 Edwards, California 93523-0273				8. PERFORMING ORGANIZATION REPORT NUMBER H-2427
9. SPONSORING/MONITORING AGENCY NAME(S) AND ADDRESS(ES) National Aeronautics and Space Administration Washington, DC 20546-0001				10. SPONSORING/MONITORING AGENCY REPORT NUMBER NASA/TP-2000-209034
11. SUPPLEMENTARY NOTES Robert D. Quinn, Analytical Services and Materials, Inc., Edwards, California; Leslie Gong, NASA Dryden Flight Research Center, Edwards, California.				
12a. DISTRIBUTION/AVAILABILITY STATEMENT Unclassified—Unlimited Subject Category 34 This report is available at http://www.dfrc.nasa.gov/DTRS/				12b. DISTRIBUTION CODE
13. ABSTRACT (Maximum 200 words) This report describes a method that can calculate transient aerodynamic heating and transient surface temperatures at supersonic and hypersonic speeds. This method can rapidly calculate temperature and heating rate time-histories for complete flight trajectories. Semi-empirical theories are used to calculate laminar and turbulent heat transfer coefficients and a procedure for estimating boundary-layer transition is included. Results from this method are compared with flight data from the X-15 research vehicle, YF-12 airplane, and the Space Shuttle Orbiter. These comparisons show that the calculated values are in good agreement with the measured flight data.				
14. SUBJECT TERMS Aerodynamic heating, Boundary layer, Flight measurements, Flow hypersonic, Flow inviscid				15. NUMBER OF PAGES 36
				16. PRICE CODE A03
17. SECURITY CLASSIFICATION OF REPORT Unclassified	18. SECURITY CLASSIFICATION OF THIS PAGE Unclassified	19. SECURITY CLASSIFICATION OF ABSTRACT Unclassified	20. LIMITATION OF ABSTRACT Unlimited	